Stable Gold Nanoparticles: Preparation, Optimization, Melatonin Loading and Enhanced Cytotoxicity

Mona Elhabak[1,2*], Rihab Osman[1], Gehanne A.S. Awad[1], Nahed D. Mortada[1]

[1]:*Faculty of Pharmacy, Ain Shams University, P.O. Box 11566, Cairo, Egypt.*

[2]*Al-ahram Canadian University, Egypt.*

ABSTRACT

The aim of the present study was the loading and characterization of Melatonin on Gold nanoparticles to be used as an adjuvant for breast cancer therapy to protect against the side effects of radiotherapy, chemotherapeutic drugs, and to potentiate their oncostatic effects. Citrate gold nanoparticles were first prepared according to Turkevich method. Loading of Melatonin on gold nanoparticles was done by direct adsorption method. The effect of loading time and the amount of Melatonin loaded were studied. Then gold nanoparticles were characterized for Ultraviolet spectroscopic analysis, FTIR, surface morphology by TEM, size, PDI and zeta potential, % EE, stability in phosphate buffer of pH 7.4 at different molarities, *in-vitro* drug release study and *in-vitro* cell viability (%). Melatonin loading by adsorption method was obvious after 2 h incubation by the shift and decrease in the SPR of gold nanoparticles and the appearance of new band between 600 and 650 nm. The increases in loading time lead to significant decrease in % EE. Melatonin loading was confirmed by FTIR, TEM and the increase in PS from 36.83 ± 0.71 to 57.64 ± 0.95 and the decrease in ζ from -32.2 to -20 (mV) for gold nanoparticles and Melatonin-gold nanoparticles, respectively. *In-vitro* release study showed enhanced Melatonin release. Melatonin-gold nanoparticles were stable in phosphate buffer of pH 7.4 up to 0.025M. Plain gold nanoparticles, free Melatonin and Melatonin-gold nanoparticles demonstrated cell viability of 90, 44.7 & 41.9%, respectively.

INTRODUCTION

Cancer is the leading cause of death worldwide with breast cancer being one of the top occurring types of cancer around the world with high mortality rate[1]. Presently, treatments of breast cancer are limited to chemotherapy, radiation and surgery. Due to inadequate therapies and clinical procedures for overcoming multi-drug resistant cancer with the severe side effects caused by systemically delivered drugs, it is vital that new technologies emerge for accurate early detection and treatment of breast cancer[2].Gold nanoparticles (GNPs) represent a versatile, potent, selective and highly multi-functional anti-cancer technology. They are characterized by particular and unique physical, chemical and photonic properties. The core of gold is chemically inert and non-toxic[3]and NPs can be easily synthesized with tunable shape and size ranging from 1 to 150 nm. By changing the size, shape and surface of GNPs, the wavelength of their plasmon absorption can be tuned to coincide in the near-IR (NIR) window (~650–900 nm), where penetration of 10 cm in depth through breast tissue even at low laser power densities can be achieved[4]. In those spectral regions, the attenuation of photons by tissues and physiological fluids is minimal and the increase in the local temperature using laser photothermal therapy (PTT) is sufficient to induce rapid tumor cell death (necrosis) with minimal damage to surrounding tissues[4]. Also, the attractive optical and electronic properties of GNPs themselves or of the GNPs co-labeled with imaging contrast agents can be used as radiation therapy, biosensing, photo-imaging and spectrochemical diagnostic contrasting diverse areas such as *in-vitro* assays, *in-vitro* and *in-vivo* non-invasive imaging[5]. GNPs are characterized by large surface area to volume ratio that allows for efficient loading of drugs and targeting ligands [6].Conjugation of small drug molecules or large biomolecules, like proteins, DNA or RNA, to GNPs can be achieved by either adsorption or chemical interactions. Adsorption is helped by either ionic interactions between negative charged GNPs and positively charged molecules or hydrophobic interaction between gold surface and hydrophobic part of drug or targeting moiety [7].Chemical interactions or covalent conjugation is achieved through the use of thiol derivatives, bifunctional linkers or adapter molecules[7].Conjugation is generally confirmed by the increase in the hydrodynamic diameter (HD) of the NPs after coupling. GNPs have the advantage over conventional liposomes and poly(lactic-*co*-glycolic acid) NPs by the ability of surface functionalisation with active ligands at densities of ($1.0 \times 106 \ \mu m^{-2}$) which is 100- and 1000-fold higher, respectively [8].

Citation: Mona Elhabak et al. Ijppr.Human, 2017; Vol. 9 (2): 107-123.
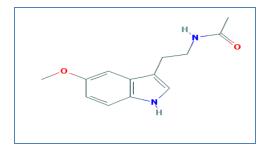
108

As nanocarriers, they suffer from non-specific uptake and potential degradation in macrophages. Surface covering of GNPs with biocompatible polymers as PEG elicits low immunogenic responses and longer circulatory half-lives[9]. Targeting is important for maximizing drug efficacy and minimizing side effects. Targeting of GNPs is achieved by passive targeting, active targeting, or a combination of both strategies to achieve tumor-specific particle accumulation. Size-selective accumulation at tumor sites due to the enhanced permeability and retention effect is a particular advantage of anti-cancer GNPs[10]. Active targeting is achieved by conjugating GNPs with various tumor-targeting agents, such as antibodies, peptides, and small molecules such as folic acid.Once accumulated in tumor tissue, GNPs enter the cell, by an energy-dependent process, mainly by endocytosis. Cellular uptake is dependent on charge, surface chemistry, size and shape. Studies showed that 50 nm citrate-capped spherical GNPs exhibited optimal uptake[11].

Various methods have been developed for the synthesis of GNPs including chemical, physical and biological methods. Turkevich method is a commonly used method for synthesis of spherical GNPs in the size range of 10-20 nm. The principle of this method involves reduction of gold ions (Au^{3+}) to gold atoms (Au^0) in the presence of reducing agents like citrate, amino acids, ascorbic acid or UV light[12]. GNPs are further stabilized using various capping agents.TheBrust method is used to produce spherical GNPs (1-3nm) in organic liquids immiscible with water. It is a two phase process in which gold salt is transferred from aqueous solution to an organic solvent as toluene using tetraoctylammonium bromide (TOAB) as phase transfer agent followed by gold reduction using sodium borohydride ($NaBH_4$) in the presence of dodecanethiol[13]. Seeding growth method is applied to obtain GNPs in other shapes such as rods, cubes, tubes. Gold seed particles are first produced by reducing gold chloride solution using a strong reducing agent like sodium borohydride. Then formed gold seed particles are added as catalyst to a solution of Au chloride containing ascorbic acid (weak reducing agent) and cetyltrimethylammonium bromide (CTAB) (structure directing agent to accelerate the anisotropic growth of GNPs)[14]. Green synthesis of GNPs is using plants extracts and microorganisms for the reduction of gold. This method has the advantage of being clean, eco-friendly and non-toxic[15].From all the above methods of GNPs preparations, the Turkevich reduction method is considered the most representative and popularly used procedure to synthesize GNPs, because of its simplicity, reproducibility and the loose shell of citrates on the NP surfaces which are easily replaced by

Citation: Mona Elhabak et al. Ijppr.Human, 2017; Vol. 9 (2): 107-123.

109

other desired ligands with valuable function[16].Although the nano surface of GNPs prepared by Turkevisch method [17]showed overall negative charge, no decrease in uptake was found. The negative citric acid groups desorb from the NP surface by nonspecific adsorption of serum proteins and were replaced by high concentrations of positive primary and secondary amines on the NP surface which allow for uptake to take place[4].

GNP scan is used to deliver drugs and imaging agents that exhibit low solubility, poor pharmacokinetics, poor intracellular penetration (e.g., siRNA) or those that are susceptible to enzymatic degradation[18].

Melatonin (Mel), structure Figure 1, N-acetyl-5-methoxytryptamine, is an indolic compound secreted mainly by the pineal gland during the dark hours at night. Secretion of Mel downregulates the gonadal activity, then any reduction in melatonin synthesis, whatever its cause, could lead to a relative increase in estrogen levels [19]. As estrogens are involved in many aspects of the malignant process, including proliferation, angiogenesis, metastasis, immune evasion, and immortality, Melcanthus be useful in treatment of estrogen dependent tumors, particularly breast cancer. The oncostatic effect of Mel results from the reduction of estradiol level as well as the Mel-estradiol interactions at cellular level[20]. Mel affects the hypothalamic-pituitary-ovarian axis, leading to lower circulating levels of estrogen and progesterone[21].At cellular level, Mel acts as a selective estrogen receptor modulator (SERM) by decreasing estrogen receptor alpha expression and reducing the ability of estrogen-estrogen receptor alpha complex to bind to the estrogen response element on DNA. Mel also acts as a selective estrogen enzyme modulator, through the reduction of the activity of aromatase in cells, which is responsible for conversion of androgenic precursors to estrogens. Overall its effect on cancer cell is oncostatic at physiological levels and cytotoxic at higher concentrations.

Figure 1: Mel Chemical Structure

Citation: Mona Elhabak et al. Ijppr.Human, 2017; Vol. 9 (2): 107-123.

110

Mel is also a potent antioxidant and exerts a free radical scavenging activity by reducing reactive oxygen species and protecting DNA from damage[22].Mel belongs to the antioxidant group of radioprotectors and so can be used as an adjuvant with radiotherapy[23]. By delaying the saturation of the repair enzymes, it allows the repair of induced damage and the use of higher doses of radiation and so provides better therapeutic value. Mel has also been shown to have an immunomodulating activity where it had been shown that extrapineal production of Mel by lymphocytes increased the activity of interleukin-2 (IL-2) and IL-2 receptor system [24].Melsharesproperties of the selective estrogen receptor modulators (SERM), selective estrogen enzyme modulators and antioxidant compounds, without most of their side effects. It can thus be an excellent adjuvant with the drugs currently used for breast cancer treatment to give synergistic oncostatic effect and also to reduce oxidative stress and to protect from side effects associated with chemotherapeutics agents[25].

The poor stability and short half-life (45min)[26]and the limited solubility of Mel in water (0.1mg/ml)[27]make it challenge to prepare Melin aqueous solution for IV administration as adjuvant therapy to protect against the side effects of radiotherapy, chemotherapeutic drugs and, to, potentiate their oncostatic effects.

In this study, we present the loading of Mel on GNPs to increase its solubility and to protect from degradation and prolong its circulation half-life. GNPs are also expected to increase Mel accumulation in breast tumor cell by EPR effect and in its cell uptake. In future study, we will study the effect of photothermal effect of Mel loaded GNPs as synergistic effect in cancer treatment.

MATERIALS AND METHODS

MATERIALS

Melatonin (Mel) was obtained from Sunrise Ltd. (China). Chloroauric acid (HAuCl4), sodium citrate, dimethylsulfoxide (DMSO), MTT and trypan blue dye were obtained from Sigma (St. Louis, Mo., USA). Fetal Bovine serum (FBS), RPMI-1640, HEPES buffer solution, L-glutamine, gentamicin and 0.25% trypsin-EDTA were obtained from Lonza. All other chemical and solvents were of analytical grades.

Citation: Mona Elhabak et al. Ijppr.Human, 2017; Vol. 9 (2): 107-123.

111

METHODS

1. Synthesis of citrate-reduced GNPs:

GNPs were synthesized using $HAuCl_4$ and sodium citrate according to the Turkevich method[17]. Briefly, 100 mL of 0.1mM $HAuCl_4$ was boiled in a conical flask under continuous stirring. Then, 0.114 g sodium citrate dissolved in 10mLdistilled water was added and stirred while heating till a red color was obtained. The solution was allowed to cool to room temperature.

2. Preparation of Mel loaded GNPs (Mel-GNPs):

For the preparation of Mel-GNPs, a stock solution of 25mg/mL of Mel in ethanol was first prepared. An amount equivalent to 6.5mg of Melwas then added to 2 mL of GNPs colloidal solution. This solution was kept under stirring at room temperature for 2 h in a closed stoppered flask, then the lid was opened to allow for ethanol evaporation[28].The change in SPR of GNPs was determined using UV-Vis spectrophotometer.

2.1.Effect of loading time:

Different mixing times: 2, 4 & 24 h were tried and the effect on entrapment efficiency (%) was determined.

2.2.Effect of theoretical amount of loaded Mel

Different volumes of Mel stock solution in ethanol equivalent to 5, 6.5, 8 and 10 mg of Mel were tried. The effects on SPR, PS, PDI, ζ and % EE were determined.

3. GNPs characterization:

3.1. Ultraviolet spectroscopic (UV) analysis of GNPs:

The UV analysis was determined by scanning the freshly prepared GNPs and Mel-GNPs using the UV/Vis spectrophotometer (Shimadzu, Japan) in the range400-800 nm.

Citation: Mona Elhabak et al. Ijppr.Human, 2017; Vol. 9 (2): 107-123.

112

3.2.Particle size (PS), polydispersity index (PDI)and zeta potential (ζ) determination:

The average PS, PDI and ζ of NPs were measured by photon correlation spectroscopy (PCS) technique using zeta sizer (Nano ZS, Malvern Instruments Ltd., Worcestershire, UK).

4. Determination of percent entrapment efficiency (%EE):

The prepared GNPs were centrifuged at 15000 rpm in a cooling centrifuge. Drug loading was indirectly calculated by estimating the amount of Mel in the supernatant. The drug concentration in supernatant was determined by UV/Vis absorption at 278nm[29].

EE (%) = Total amount of Mel added – amount of Mel in supernatant)/ (Total amount of Mel added) × 100

5. Fourier transform infrared (FT-IR) analysis:

Fourier transform infrared (FT-IR) spectra were obtained by Thermo Nicolet Nexus spectrometer. Samples were pressed into potassium bromide (KBr) pellets and recorded at frequencies from 4000 to 200 cm^{-1} with resolution of 4 cm^{-1}.

6. Morphological characterization using transmission electron microscopy (TEM):

Both plain and Mel-GNPs were examined in Technai G2 S-TWIN and images were obtained at 120 Hz. A single drop of GNPs dispersion was deposited on a copper grid and then dried in air before imaging.

7. *In-vitro* Mel release from GNPs:

The release study was carried out using dialysis membrane of 10 kD cutoff. The NPs, dispersed in 2mLphosphate buffer solution (PBS), pH7.4, were placed inside the dialysis bag which was then tied at both ends. The bag was suspended in a beaker containing 50 mLPBS, placed in a shaker water bath at 80 stokes/min and incubated at 37˚C[30]. 1 mL of dissolution medium was withdrawn at determined time intervals and was replaced with fresh medium. Drug concentrations were determined using UV/Vis spectrophotometer at 278 nm.

Citation: Mona Elhabak et al. Ijppr.Human, 2017; Vol. 9 (2): 107-123.

113

8. Stability study:

The stability of Mel-GNPs was evaluated in PBS, pH=7.4, of different molarities namely: 0.005, 0.01, 0.025, 0.05 and 0.1 M. The change in SPR using UV/Vis spectrophotometer was recorded at 400-800 nm.

9. Cytotoxicity Study:

Mammalian cell lines: MCF-7 cells (human Breast cancer cell line), were obtained from the American Type Culture Collection (ATCC, Rockville, MD).

Cell line Propagation:

The cells were grown on RPMI-1640 medium supplemented with 10% inactivated fetal calf serum and 50µg/mL gentamycin. The cells were maintained at 37ºC in a humidified atmosphere with 5% CO2 and were subcultured two to three times a week.

Cytotoxicity evaluation using viability assay: For antitumor assays, the tumor cell lines were suspended in medium at concentration 5×10^4 cell/well in Corning® 96-well tissue culture plates, then incubated for 24 h. The tested compounds were then added into 96-well plates (three replicates) to achieve twelve concentrations for each compound. Six vehicle controls with media or 0.5 % DMSO were run for each 96 well plate as a control. After incubating for 24 h, the numbers of viable cells were determined by the MTT test. Briefly, the media was removed from the 96 well plates and replaced with 100 µL of fresh culture RPMI 1640 medium then 10 µL of MTT stock solution (5 mg of MTT in 1 mL of PBS) was added to each well including the untreated controls. The 96 well plates were then incubated at 37°C and 5% CO_2 for 4 h. The media was removed from the wells, washed with 100 µL of PBS, then100 µL of DMSO was added to each well and mixed thoroughly with the pipette and incubated at 37°C for 10 min. Then, the optical density was measured at 590 nm with the microplate reader (SunRise, TECAN, Inc, USA) to determine the number of viable cells and the percentage of viability was calculated as [1-(ODt/ODc)]x100% where ODt is the mean optical density of wells treated with the tested sample and ODc is the mean optical density of untreated cells. The relation between surviving cells and drug concentration is plotted to get the survival curve of each tumor cell line after treatment with the specified compound .The 50% inhibitory concentration (IC_{50}), the

Citation: Mona Elhabak et al. Ijppr.Human, 2017; Vol. 9 (2): 107-123.

114

concentration required to cause toxic effects in 50% of intact cells, was estimated from graphic plots of the dose response curve for each concentration using Graphpad Prism software (San Diego, CA. USA).

Statistical analysis:

All formulations were prepared and reported in triplicates. Results are expressed as mean ± SD (standard deviation). The statistical significance of difference between groups were evaluated by one-way ANOVA and Tukey's post hoc test with a significance level of $p < 0.05$.

RESULTS AND DISCUSSION

Colloidal dispersion of GNPs was prepared by the reduction and stabilization of $HAuCl_4$ with sodium citrate. The change in color from yellow to red indicated NPs formation [17]. GNPs exhibit a unique SPR invisible region[31]. The maximum wavelength for GNPs was observed at 519 nm (fig.2) which indicates small size distribution as well as good NPs stability[32].
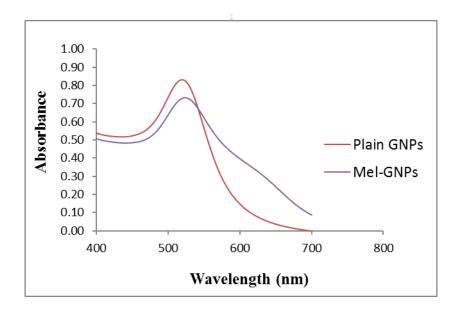

Figure 2: UV spectra of plain and Mel-GNPs

Mel loading and formation of gold aggregates were obvious by the shift and decrease in the SPR of GNPs and the appearance of new band between 600 and 650nm due to plasmon coupling of NPs as shown in fig (2)[28].This was also confirmed by the change of color from ruby to purple.

Citation: Mona Elhabak et al. Ijppr.Human, 2017; Vol. 9 (2): 107-123.

115

Different mixing times were tried for loading 6.5mg Mel on GNPs: 2, 4 & 24 h and the EE % was found to be 60.49±1.37, 24.05±1.18, 6.49±2.41% (w/w), respectively as shown in Table 1. The increase in loading time of Mel on GNPs had a significant effect on decreasing the %EE. Desorption of the drug from the surface of GNPs resulted in this decrease in drug loading and hence 2 h was selected for further experiments.

Table 1: Effect of loading time on percent drug loaded on GNPs

Time (h)	Mel loaded (% w/w)
2	60.49±1.37
4	24.05±1.18
24	6.49±2.41

All results are expressed as mean of three measurements ±SD. A theoretical Mel loading of 6.5 mg was used.
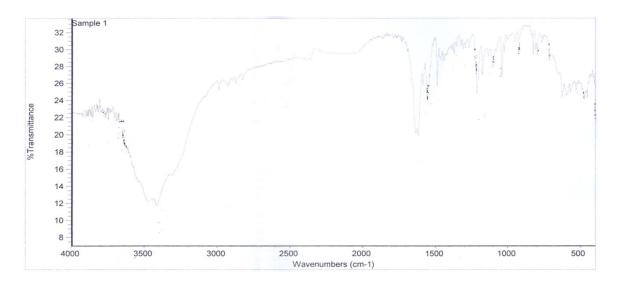
The average hydrodynamic diameter of GNPs was found to be 36.83±0.71 nm with a PDI of 0.559±0.03. Table (2) shows a significant ($p< 0.05$) increase in PS with increase drug loading up to 6.5mg beyond which no further increase in PS was seen. ζ of plain GNPs was found to be -32.2 (mV), we observed decrease in ζ to -20 (mV) after loading with 6.5mg melatonin denoting that the drug cationic amine group reduced citrate carboxyl group. No significant change was then seen by further increasing Mel amount as shown in table (2). These results were confirmed by determination of %EE of Mel on GNPs(table 2).EE for 5, 6.5, 8 and 10 mg Mel were 56.26±2.61, 60.49±1.37, 52.9±1.99, 49.1±2.76 %, respectively. The increase in Mel amount from 5 to 6.5 mg showed a significant increase %EE, while further increase in Mel theoretical loading was accompanied by significant decrease in % EE.
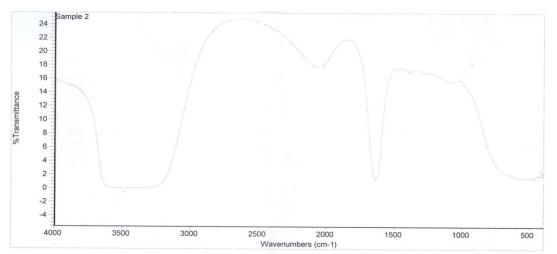
Citation: Mona Elhabak et al. Ijppr.Human, 2017; Vol. 9 (2): 107-123.

116

Table 2: Effect of amount of Mel on PS, PDI, ζ and %EE

Melatonin amount (mg)	Mean P.S (nm)	PDI	ζ (mV)	% EE (w/w)
Plain GNPs	36.83±0.71	0.559±0.03	-32.2±2.37	-
5	46.64±1.20	0.607±0.00	-26.0±1.81	56.26±2.61
6.5	57.64±0.95	0.502±0.01	-20.0±2.21	60.49±1.37
8	60.43±2.10	0.474±0.02	-19.9±0.65	52.90±2.00
10	53.53±1.60	0.481±0.01	-20.2±1.32	49.10±2.76

All results are expressed as mean of three measurements ±SD.

The FT-IR spectra of citrate-AuNPs, Figure 3 (b), depicts characteristic bands of citrate at 3527.83 and1635.62cm^{-1}. The first was assigned to the stretching vibration of OH group and the later was indicative of C=O stretching of citrate carboxylate ions[33].From the FT-IR spectrum of Mel, two sharp bands between 3500 and 3414.32 cm^{-1}of Mel assigned to indolic and amidic NH stretching respectively could be observed. The band at 1085-1150cm^{-1}was due to C-O-C stretch, while the bands at 1450-1600 cm^{-1}was due to ring C=C stretch, and those at 2850-3000 was due to C-H stretch of alkane group. The band at 1618.45 was indicative of C=O stretching Figure 3 (a)[15].Drug loading onto GNPs was achieved through electrostatic attraction between Mel cationic amine group and anionic carboxyl groups of citrate. This was evidenced by the FT-IR analysis. A shift of the characteristic band at 3527.83cm^{-1}of gold citrate corresponding to the hydroxyl group to 3452.2 cm^{-1}withthe disappearance of the 1618.45cm^{-1} peak of Mel corresponding to its C=O stretching. Possibility of hydrogen bonding, in addition to electrostatic interaction between protonated amine group and anionic GNPs, Figure 3 (c), is probably responsible for the drug loading onto GNPs.
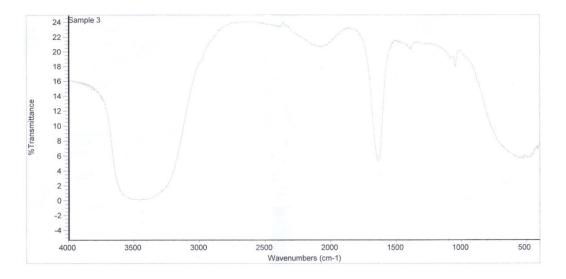
Citation: Mona Elhabak et al. Ijppr.Human, 2017; Vol. 9 (2): 107-123.

117

Figure 3: FT-IR spectra of (a) Mel, (b) Plain GNPs and (c) Mel-GNPs

Citation: Mona Elhabak et al. Ijppr.Human, 2017; Vol. 9 (2): 107-123.

118

TEM image in Figure 4 (a) shows spherical, non-aggregated small NPs with in accordance with PCS data. The aggregation, seen in Figure 4 (b), confirmedMel loading on GNPs.
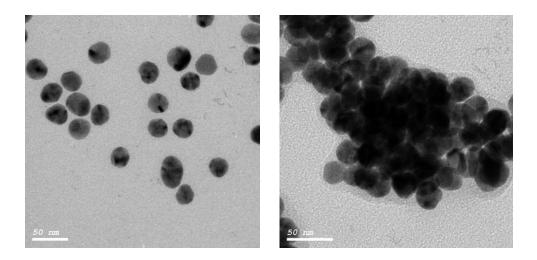

Figure (4): TEM of (a) GNPs and (b) Mel-GNPs

As could be depicted from Figure 5, Mel release was greatly enhanced following loading onto GNPs: 89.1% w/w of Mel were leased within 2 h.
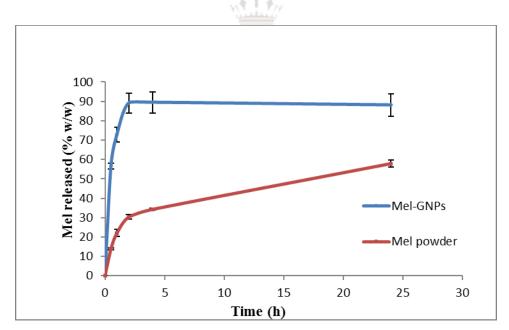

Figure 5: Mel release profile from GNPs in PBS pH=7.4, 37°C and 80 stokes/min

Citation: Mona Elhabak et al. Ijppr.Human, 2017; Vol. 9 (2): 107-123.

119

Stability study results in Figure 6, showed no change in spectra of Mel-GNPs in PBS of molarity lower than0.025 M. In contrast to the shift noticed at higher ionic strengths, 0.05 and 0.1M to longer wavelength proving the stability of GNPsin PBS up to 0.025M.
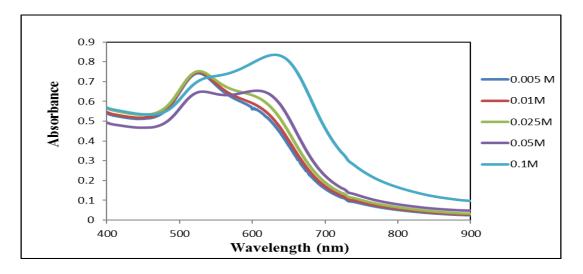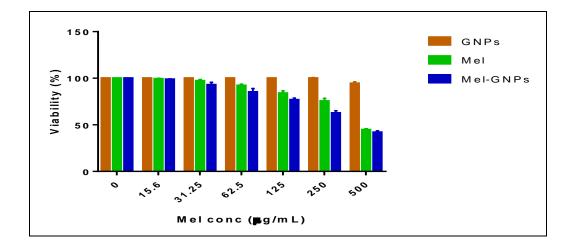

Figure 6: Effect of PBS ionic strength on Mel-GNPs stability

Inhibitory activity against breast carcinoma cells was detected using MTT assay, Figure 7. In accordance with the results found by previous investigators, plain GNPs exhibited cell viability close to 90%, suggesting that plain GNPs had no significant cytotoxic effects. On the other hand, free Mel and Mel-GNPs demonstrated cell viability of 44.7 and41.9%respectively, which indicate that it has minor cytotoxic effects. In contrast, the cell viability decreased significantly to 41.9% when incubated with Mel-GNPs.

Figure 7: MTT assay of GNPs, Mel powder and Mel-GNPs on MCF-7 breast cells.

Citation: Mona Elhabak et al. Ijppr.Human, 2017; Vol. 9 (2): 107-123.

120

Plain GNPs was used to in an equivalent amount to that containing the corresponding Mel concentration.

CONCLUSION

This Study showed the feasibility of loading Mel on GNPs by direct adsorption method. Loading 6.5 mg of Mel per mL of GNPs (0.001M) for 2h gave optimum results. Mel-GNPs showed enhanced Mel release, excellent NPs stability in PBS up to 0.025M and enhanced cytotoxicity on breast cancer cells. Mel-GNPs could thus be formulated as IV dosage forms to be given as adjuvant therapy in breast cancer treatment to combine between the oncostatic and radioprotective effect of Mel and synergistic photothermal effect of GNPs.

FINANCIAL SUPPORT AND SPONSORSHIP

Nil.

CONFLICTS OF INTEREST

There are no conflicts of interest

REFERENCES

1. Ferlay J, Soerjomataram I, Dikshit R, Eser S, Mathers C, Rebelo M, et al. Cancer incidence and mortality worldwide: sources, methods and major patterns in GLOBOCAN 2012. International journal of cancer. 2015;136(5): E359-E86.
2. Arvizo R, Bhattacharya R, Mukherjee P. Gold nanoparticles: opportunities and challenges in nanomedicine. Expert opinion on drug delivery. 2010;7(6):753-63.
3. Han G, Ghosh P, Rotello VM. Multi-functional gold nanoparticles for drug delivery. Bio-applications of Nanoparticles: Springer; 2007. p. 48-56.
4. Dreaden EC, Austin LA, Mackey MA, El-Sayed MA. Size matters: gold nanoparticles in targeted cancer drug delivery. Therapeutic delivery. 2012;3(4):457-78.
5. Cai W, Gao T, Hong H, Sun J. Applications of gold nanoparticles in cancer nanotechnology. Nanotechnology, science and applications. 2008;2008(1).
6. Wang J, Zhang G, Li Q, Jiang H, Liu C, Amatore C, et al. In vivo self-bio-imaging of tumors through in situ biosynthesized fluorescent gold nanoclusters. Scientific reports. 2013;3:1157.
7. Jazayeri MH, Amani H, Pourfatollah AA, Pazoki-Toroudi H, Sedighimoghaddam B. Various methods of gold nanoparticles (GNPs) conjugation to antibodies. Sensing and Bio-Sensing Research. 2016;9:17-22.
8. Park J, Mattessich T, Jay SM, Agawu A, Saltzman WM, Fahmy TM. Enhancement of surface ligand display on PLGA nanoparticles with amphiphilic ligand conjugates. Journal of controlled release. 2011;156(1):109-15.
9. Owens DE, Peppas NA. Opsonization, biodistribution, and pharmacokinetics of polymeric nanoparticles. International journal of pharmaceutics. 2006;307(1):93-102.

Citation: Mona Elhabak et al. Ijppr.Human, 2017; Vol. 9 (2): 107-123.

121

10. Maeda H, Wu J, Sawa T, Matsumura Y, Hori K. Tumor vascular permeability and the EPR effect in macromolecular therapeutics: a review. Journal of controlled release. 2000;65(1):271-84.

11. Murugan K, Choonara YE, Kumar P, Bijukumar D, du Toit LC, Pillay V. Parameters and characteristics governing cellular internalization and trans-barrier trafficking of nanostructures. International journal of nanomedicine. 2015;10:2191.

12. Shah M, Badwaik V, Kherde Y, Waghwani HK, Modi T, Aguilar ZP, et al. Gold nanoparticles: various methods of synthesis and antibacterial applications. Front Biosci. 2014;19(1320):10.2741.

13. Brust M, Walker M, Bethell D, Schiffrin DJ, Whyman R. Synthesis of thiol-derivatised gold nanoparticles in a two-phase liquid–liquid system. Journal of the Chemical Society, Chemical Communications. 1994 (7):801-2.

14. Hedkvist O. Synthesis and Characterization of Gold Nanoparticles. 2013.

15. Singh P, Kim Y-J, Zhang D, Yang D-C. Biological synthesis of nanoparticles from plants and microorganisms. Trends in biotechnology. 2016;34(7):588-99.

16. 16. Khaled, A., Mohamed, A., Wael, A., Gamal, Z. , Montasser, S. & Mohamed, S. 2016.Synthesis and characterization of gold nanoparticles loaded with 5-Fluorouracil. IJPPR, 6, 3.

17. Turkevich J, Stevenson PC, Hillier J. A study of the nucleation and growth processes in the synthesis of colloidal gold. Discussions of the Faraday Society. 1951;11:55-75.

18. Giljohann DA, Seferos DS, Prigodich AE, Patel PC, Mirkin CA. Gene regulation with polyvalent siRNA-nanoparticle conjugates. Journal of the American Chemical Society. 2009;131(6):2072.

19. Hardeland R, Cardinali DP, Srinivasan V, Spence DW, Brown GM, Pandi-Perumal SR. Melatonin—A pleiotropic, orchestrating regulator molecule. Progress in neurobiology. 2011;93(3):350-84.

20. D Mediavilla M, J Sanchez-Barcelo E, X Tan D, Manchester L, J Reiter R. Basic mechanisms involved in the anti-cancer effects of melatonin. Current medicinal chemistry. 2010;17(36):4462-81.

21. Voordouw B, Euser R, Verdonk RE, Alberda BT, de Jong FH, Drogendijk AC, et al. Melatonin and melatonin-progestin combinations alter pituitary-ovarian function in women and can inhibit ovulation. The Journal of Clinical Endocrinology & Metabolism. 1992;74(1):108-17.

22. Karbownik M, Lewinski A, Reiter RJ. Anticarcinogenic actions of melatonin which involve antioxidative processes: comparison with other antioxidants. The international journal of biochemistry & cell biology. 2001;33(8):735-53.

23. Shirazi A, Ghobadi G, Ghazi-Khansari M. A radiobiological review on melatonin: a novel radioprotector. Journal of radiation research. 2007;48(4):263-72.

24. Carrillo-Vico A, Lardone PJ, Fernández-Santos JM, Martín-Lacave I, Calvo JR, Karasek M, et al. Human lymphocyte-synthesized melatonin is involved in the regulation of the interleukin-2/interleukin-2 receptor system. The Journal of Clinical Endocrinology & Metabolism. 2005;90(2):992-1000.

25. Cohen M, Lippman M, Chabner B. Role of pineal gland in aetiology and treatment of breast cancer. The Lancet. 1978;312(8094):814-6.

26. Harpsøe NG, Andersen LPH, Gögenur I, Rosenberg J. Clinical pharmacokinetics of melatonin: a systematic review. European journal of clinical pharmacology. 2015;71(8):901-9.

27. Zieliński H, Szawara-Nowak D, Wiczkowski W. Determination of melatonin in bakery products using liquid chromatography coupled to tandem mass spectrometry (LC–MS/MS). Chemical Papers.1-7.

28. Mohamed M, Adbel-Ghani N, El-Borady O, El-Sayed M. 5-Fluorouracil induces plasmonic coupling in gold nanospheres: new generation of chemotherapeutic agents. Journal of Nanomedicine and Nanotechnology. 2012;3(7):1-7.

29. Girgin B, Korkmaz O, Yavaşer R, Karagözler AA. Production and Drug Release Assesment of Melatonin-Loaded Alginate/Gum Arabic Beads. Journal of the Turkish Chemical Society, Section A: Chemistry. 2016;3(3):205-16.

30. 30. Grumezescu A. Nutraceuticals: Academic Press; 2016.

31. Huang X, El-Sayed MA. Gold nanoparticles: optical properties and implementations in cancer diagnosis and photothermal therapy. Journal of Advanced Research. 2010;1(1):13-28.

Citation: Mona Elhabak et al. Ijppr.Human, 2017; Vol. 9 (2): 107-123.

122

32. Lata K, Jaiswal AK, Naik L, Sharma R. Gold Nanoparticles: Preparation, Characterization and Its Stability in Buffer. Nano Trends: A Journal of Nanotechnology and Its Application. 2014;17(1):1-10.

33. Kiroula N, Negi J, Singh K, Rawat R, Singh B. Preparation and Characterization of Ganciclovir-loaded Glutathione Modified Gold Nanoparticles. Indian Journal of Pharmaceutical Sciences. 2016;78(3):313-9.

HUMAN

Citation: Mona Elhabak et al. Ijppr.Human, 2017; Vol. 9 (2): 107-123.

123